Atmos. Chem. Phys. Discuss., https://doi.org/10.5194/acp-2018-1148
Manuscript under review for journal Atmos. Chem. Phys.
Discussion started: 11 December 2018

Atmospheric Chemistry and Physics Discussions

Inter-comparison of O_3 formation and radical chemistry in the past decade at a suburban site in Hong Kong

Xufei Liu[1,#], Xiaopu Lyu[1,#], Yu Wang[1], Fei Jiang[2], Hai Guo[1,*]

[1] Air Quality Studies, Department of Civil and Environmental Engineering, The Hong Kong Polytechnic University, Hong Kong, China

[2] Jiangsu Provincial Key Laboratory of Geographic Information Science and Technology, International Institute for Earth System Science, Nanjing University, Nanjing, China

*Corresponding author. ceguohai@polyu.edu.hk

# Both authors made equal contribution.

Abstract

Hong Kong, as one of the densely populated metropolises in East Asia, has been suffering from severe photochemical smog in the past decades, though the observed nitrogen oxides (NO_x) and total volatile organic compounds (TVOCs) were significantly reduced. This study, based on the observation data in the autumns of 2007, 2013 and 2016, investigated the photochemical ozone (O_3) formation and radical chemistry during the three sampling periods in Hong Kong with the aid of a Photochemical Box Model incorporating the Master Chemical Mechanism (PBM-MCM). Neither the observed O_3 nor the simulated locally produced O_3 changed significantly (p=0.11 and 0.99, respectively) from 2007 to 2013; however, both of which decreased (p<0.05) from the VOC sampling days in 2013 to those in 2016 at a rate of -5.04±0.05 and -4.35±0.10 ppbv yr^{-1}, respectively. The regionally transported O_3 showed an increase (rate = 1.62±0.39 ppbv yr^{-1}, p<0.05) during 2007-2013, but slight decrease (p=0.09) from 2013 to 2016. The mitigation of autumn O_3 pollution in this region was further confirmed by the continuous monitoring data, which has never been reported in previous studies. Benefited from the air pollution control measures taken in Hong Kong, the local O_3 production rate decreased remarkably (p<0.05) from 2007 to 2016, along

with the lowering of recycling rate of hydroxyl radical (OH). Specifically, VOCs emitted from the source of liquefied petroleum gas (LPG) usage and gasoline evaporation decreased in this decade at a rate of -2.61±0.03 ppbv yr^{-1}, leading to a reduction of the O_3 production rate from 0.51±0.11 ppbv h^{-1} in 2007 to 0.10±0.02 ppbv h^{-1} in 2016. In addition, solvent usage made decreasing contributions to both VOCs (rate = -2.29±0.03 ppbv yr^{-1}) and local O_3 production rate (1.22±0.17 and 0.14±0.05 ppbv h^{-1} in 2007 and 2016, respectively) in the same period. All the rates reported here were for the VOC sampling days in the three sampling campaigns. It is noteworthy that meteorological changes also play important roles in the inter-annual variations of the observed O_3 and the simulated O_3 production rates. Evaluations with more data in longer periods are therefore recommended. The analyses on the decadal changes of the local and regional photochemistry in Hong Kong in this study may be a reference for combating China's national-wide O_3 pollution in near future.

Keywords: Ozone formation; Volatile organic compounds; Radical chemistry; Source apportionment; Control measures

1 Introduction

Ground-level ozone (O_3) is one of the most representative air pollutants in photochemical smog, produced through photochemical reactions between volatile organic compounds (VOCs) and nitrogen oxides (NO_x) in presence of sunlight (NRC, 1992; Jacob et al., 1999; Guo et al., 2017). It is well documented that O_3 is harmful to human health (Bell et al., 2004), crops (Wang et al., 2005) and natural ecosystems (Ashmore, 2005). Through the last 30 years, extensive efforts have been made by the local and federal governments to alleviate the tropospheric O_3 pollution around the world (NRC, 1992; NARSTO, 2000; Wang et al., 2017a; Wang et al., 2018a). Effectiveness has gradually shown in some countries/regions, such as

Switzerland, Germany, Ireland and eastern North America (Lefohn et al., 2010; Cui et al., 2011; Derwent et al., 2013; Parrish et al., 2014; Lin et al., 2017). In contrast, the O_3 levels in many places are still increasing or not decreasing at the expected rates, particularly in East Asia (Ding et al., 2008; Xu et al., 2008; Parrish et al., 2014; Xue et al., 2014a; Wang et al., 2017a).

Hong Kong, as one of the densely populated metropolises in East Asia, has been suffering from severe photochemical smog in the past decades, though the locally-emitted NO_x and total VOCs (TVOCs) were significantly reduced (Xue et al., 2014a; Ou et al., 2015; Lyu et al., 2016a; Wang et al., 2017a). On one hand, this indicates the non-linear relationship between O_3 and its precursors. On the other hand, in addition to local O_3 formation, the observed O_3 in Hong Kong is also influenced by the regional transport due to the proximity of the highly industrialized Pearl River Delta (PRD) region. Earlier studies revealed that the local O_3 production is typically limited by VOCs in urban and some suburban areas in Hong Kong (Zhang et al., 2007; Ling et al., 2014; Wang et al., 2017b). Namely, cutting VOCs emissions will reduce O_3 production, while the reduction of NO_x may cause an O_3 increment (Cheng et al., 2010, 2013; Guo et al., 2011; Wang et al., 2017a). Previous studies also documented that photochemical O_3 formation is dependent upon the ratios between TVOCs and NO_x (Sillman, 1999; Guo et al., 2013; Ling et al., 2013), reactivity of VOC species (Zhang et al., 2007; Liu et al., 2008; Cheng et al., 2010) and the composition of NO_x (*i.e.* relative abundances of NO_2 and NO) (Richter et al., 2005; Xu et al., 2008; Wang et al., 2018a). Moreover, located in the subtropical region, Hong Kong has relatively high temperature and strong solar radiation, which are favourable for local O_3 formation. For regional transport, studies (Wang et al., 2001; Ding et al., 2004; Wang et al., 2017b) indicated that O_3 was generally built up in Hong Kong under the northerly winds, whereas it was often driven down by the sea breeze from South China Sea (SCS) and by the southwest monsoon in warm seasons. The contribution of

regional transport to O_3 in Hong Kong even reached 70% under the dominance of tropical cyclone (Huang et al., 2005), a typical synoptic condition conducive to severe O_3 pollution in the Northern Hemisphere (So and Wang, 2003; Huang et al., 2005; Lam et al., 2005). To improve the air quality in Hong Kong, a series of control measures aiming at restriction of VOC emissions have been implemented by Hong Kong government since 2007, which effectively reduced the concentrations of some VOCs, such as propane and *i*-/*n*-butanes emitted from taxis and public light buses fuelled by liquefied petroleum gas (LPG) (Lyu et al., 2016b), the aromatics mainly attributable to solvent usage, and the alkenes in association with diesel exhaust (Lyu et al., 2017a). As a result, Xue et al. (2014a) and Wang et al. (2017a) found that the locally produced O_3 decreased. However, the regional and super-regional transport of O_3 and its precursors from PRD and eastern China to Hong Kong had offset the decrease of the local O_3 production, resulting in an overall increase of the observed O_3 in Hong Kong from 2005 to 2013.

Despite many previous studies (Xue et al., 2014a, 2016; Ou et al., 2015; Lyu et al., 2016a; Wang et al., 2017a; Wang et al., 2018a), the inter-annual variations of the O_3 formation regimes and radical chemistry have yet been fully understood in Hong Kong. Additionally, the online measurement data used in previous long-term O_3 study might hamper the exact understanding of the local O_3 formation mechanisms, due to the unavailability of many reactive VOCs, such as formaldehyde. Besides, the trends of the local production and regional transport of O_3 were only updated to 2013 in previous studies (Xue et al., 2014a; Wang et al., 2017a). In fact, many measures were taken to reduce air pollutants' emissions in the latest years in Hong Kong and PRD. For examples, nearly 75% of the old catalytic converters on LPG-fuelled vehicles were renewed during September 2013 - May 2014. A program to eliminate the pre-Euro IV diesel vehicles or to upgrade their emission standards to Euro IV was initiated in March 2014 and is still ongoing till 2019 at its third phase. In PRD,

the second stage of the clean air controlling program was implemented in 2013 - 2015 (DGEPD, 2013). In 2014, the Guangdong provincial government has launched an Action Plan for Air Pollution Prevention and Control (MEE PRC, 2014), putting the emphases on the emission control of traffics, coal-fired power plants and industrial sources. Investigations on the post-2013 variations of the local O_3 production in Hong Kong and the regional impacts provide a good opportunity for us to examine the effectiveness of these local and regional measures.

The objectives of this study were to re-examine the O_3 trend in the pre-2013 and trace the O_3 evolution in the post-2013 in Hong Kong, and to explore the underlying mechanisms for the variations of O_3 formation and radical chemistry. With the aid of a photochemical box model, the locally-produced and regionally-transported O_3, as well as their variation trends, were determined. Under the assumption that the local O_3 production in these years was changed due to a series of control measures in Hong Kong, we also aimed to evaluate the actual effectiveness of these control measures. China is suffering from severe O_3 pollution, almost second to none over the world. While O_3 began to decrease in most areas of North America and Europe, China's O_3 pollution was even aggravated in recent years. A series of air pollution control strategies have been implemented in China, though most of them were not specifically designed for O_3 abatement. Investigations on O_3 trends and the potential causes in Hong Kong would provide a good example of assessing the evolution of O_3 pollution and the effects of artificial interventions in China. In addition, the changes in the regional contribution to O_3 in Hong Kong determined in this study would throw light upon the variations of O_3 in China, particularly in South China. It is expected that this study would have some inspiration to the O_3 pollution control in other cities and regions in China.

2 Methodolgy

Atmos. Chem. Phys. Discuss., https://doi.org/10.5194/acp-2018-1148
Manuscript under review for journal Atmos. Chem. Phys.
Discussion started: 11 December 2018

124 **2.1 Sampling site**

125 Hong Kong is located on the southern coast of China with Guangdong province to the north
126 and Pearl River Estuary (PRE) to the northwest. The sampling site (22.29N, 113.94E), Tung
127 Chung (TC), was in a newly-developed suburban area in western Hong Kong, with a
128 population of ~77,400 in 2016 (CSD, 2011, 2018). The urban centre of Hong Kong is ~20 km
129 northeast of TC. Hong Kong is dominated by the subtropical oceanic monsoon climate.
130 During warm seasons, the prevailing winds mainly come from SCS at a relatively low speed
131 (southwest winds). In cold seasons, the east and northeast winds are predominant. Generally,
132 the sampling site receives relatively polluted air masses from mainland China, *i.e.* PRD
133 region, Yangtze River Delta region and even North China between October and March, when
134 high O_3 levels are often observed (Wang et al., 2009). Therefore, the samplings were mainly
135 conducted in October and November in this study, except for 4 out of 45 sampling days in
136 September. The sampling site was close to a highway linking to the Hong Kong International
137 Airport (HKIA), and the HKIA was around 3 km to the north of the site. In addition, the local
138 emissions from residential activities may modulate the air quality at this site. Figure 1 shows
139 the locations of the sampling site (TC) and the 12 air quality monitoring stations in PRD,
140 which witnessed the evolution of air quality in PRD over the last decade and is used to
141 demonstrate the variations of regional O_3 in this study. More detailed description of the site
142 can be found in our previous studies (Jiang et al., 2010: Cheng et al., 2010; Ling et al., 2013;
143 Ou et al., 2015).

Atmos. Chem. Phys. Discuss., https://doi.org/10.5194/acp-2018-1148
Manuscript under review for journal Atmos. Chem. Phys.
Discussion started: 11 December 2018

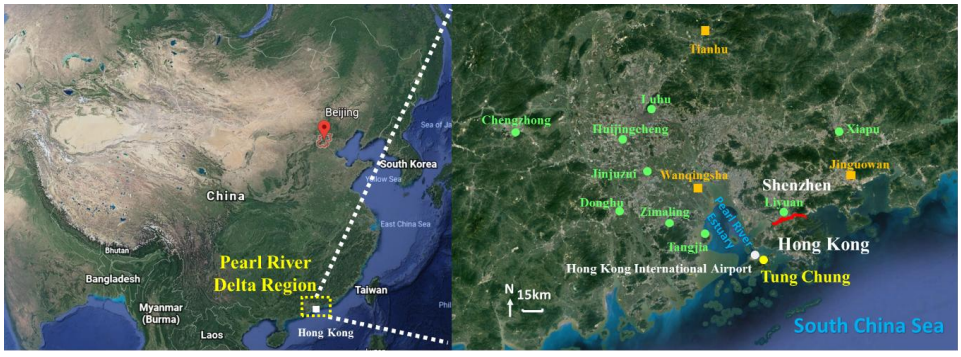

Figure 1. Location of the sampling site (yellow circle) and the surrounding environment. The red line in the right panel shows the border between Hong Kong and Shenzhen, Guangdong. The three regional and nine urban air quality monitoring stations in PRD are symbolized by orange blocks and green circles, respectively.

2.2 Continuous measurements of trace gases and collection of VOC/OVOC samples

Trace gases (SO_2, CO, NO, NO_2 and O_3) and meteorological conditions were continuously measured at TC site for three autumn periods in 2007, 2013 and 2016 (see Table S1 for the specific sampling periods), including 25 O_3 episode days with the maximum hourly average O_3 exceeding 100 ppbv (Level II of China National Ambient Air Quality Standard) and 185 non-episode days. VOC and OVOC samples were selectively collected on 8, 19 and 18 days in 2007, 2013 and 2016, respectively (see Table S1 for the specific sampling dates). The three sampling periods were used as representatives of the autumns in the three years in this study, and the rationality will be discussed in section 3.1.

Trace gases were continuously measured at the TC air quality monitoring station operated by the Hong Kong Environmental Protection Department (HKEPD), ~0.8 km to our sampling site. The instruments were the same as those used in the US air quality monitoring program (HKEPD, 2017a). Table S2 summarizes the instruments, analysis techniques, detection limits and the time resolutions for measurements of the trace gases. The high resolution data were

collected and averaged into the hourly averages. All the analysers except O_3 analyser were zeroed daily by analysing scrubbed ambient air and calibrated every two weeks by a span gas mixture with a NIST (National Institue of Standards and Technology) traceable standard, while the O_3 analyser was calibrated using a transfer standard (Thermo Environmental Instruments (TEI) 49PS) every two weeks. Details about the quality assurance and control procedures can be found in Ling et al. (2016a). The meteorological parameters, including temperature, relative humidity, pressure, wind speed, wind direction, precipitation and solar radiation, were also continuously monitored by a mini weather station (Vantage Pro TM & Vantage Pro 2 Plus TM Weather Stations, Davis Instruments) during the sampling periods. Data were integrated into 30-minute averages by a built-in program in the weather station. The collection and analysis of VOCs and OVOCs were detailed in our previous studies (Guo et al., 2009; Wang et al., 2018b). Briefly, pre-cleaned and evacuated 2 L electropolished stainless-steel canisters were used to collect VOC samples. On O_3 episode days, one-hour sample was collected in each hour during the daytime (07:00-19:00 LT), generating 13 samples per day, while 5-7 one-hour samples were collected every other hour on non-O_3 episode days from 07:00 to 19:00 LT in the 2013 and 2016 sampling campaigns. However, 12 one-hour samples were collected on each VOC sampling day between 07:00 and 18:00 in 2007, regardless of O_3 episodes or non-episodes. The O_3 episode days were predicted prior to sampling based on weather forecast and numerical simulation of O_3. Overall, the O_3 episodes were usually associated with high temperature, strong solar radiation, low humidity, and weak or northerly winds. A total of 414 canister samples, including 96 samples in 2007, 146 samples in 2013 and 172 samples in 2016, were collected and analysed during the three sampling periods (Table S1).

In addition to VOC samples, OVOC samples were also collected on the same days as those for the collection of VOCs. Dinitrophenylhydrazine (DNPH)-silica cartridges (Waters Sep-

Pak DNPH-Silica, Milford, MA) were used to collect the OVOC samples. An ozone scrubber (Sep-Pak; Waters Corporation, Milford, MA) was connected in front of the DNPH cartridge to prevent interference of ozone. The ozone scrubber was replaced every two OVOC samples. For each OVOC sample, air was drawn to pass the O_3 scrubber and the cartridge for 2 hours (2.5 hours in 2007 sampling campaign) at a flow rate of 0.5 L min^{-1}, which was controlled by a rotameter. During the sampling periods in 2013 and 2016, 5-7 OVOC samples were collected every two hours from 06:00-20:00 LT on both O_3 episode and non-episode days. In 2007, only 2 samples were collected on non-O_3 episode days at 10:30-13:00 and 13:00-15:30, and 4 samples between 08:00 and 18:00 on O_3 episode days. In total, 275 OVOC samples (28 in 2007, 124 in 2013 and 124 in 2016) were collected and analysed in the three sampling campaigns (Table S1).

2.3 Chemical analysis

2.3.1 Analysis of VOCs

The concentrations of 48 speciated non-methane hydrocarbons (NMHCs) in the canisters were determined with an Entech Model 7100 Preconcentrator (Entech Instruments Inc., California, USA) coupling with a gas chromatography-mass selective detector (Model 5973N, Agilent Technologies, USA), a flame ionization detector, and an electron capture detector (GC-MSD/FID/ECD). The NMHCs were analysed in Donald Blake's laboratory at University of California, Irvine (UCI) for the samples collected in 2007, in Guangzhou Institute of Geochemistry (GIG), Chinese Academy of Sciences for the samples collected in 2013 and in The Hong Kong Polytechnic University (HKPolyU) for the samples collected in 2016. It should be noted that the GC-MSD/FID/ECD system in the latter two institutes was the same as that at UCI, and inter-comparisons were performed regularly among the three institutes, which showed reasonably good agreements (Ling et al., 2014; Wang et al., 2018b;

Zeng et al., 2018). Detailed information about the analysis procedures and quality assurance and control can be found in Colman et al. (2001) and Simpson et al. (2010). Table S3 summarizes the limits of detection (LoDs), precisions and accuracies of the VOC analyses in the three institutes.

The OVOC samples were stored in a refrigerator at 4℃ after sampling. For analyses of OVOCs, the cartridges were eluted slowly with 2 ml of acetonitrile into a 2-ml volumetric flask. A high-performance liquid chromatography (HPLC) system (Perkin Elmer Series 2000, MA, USA) coupled with an ultraviolet (UV) detector operating at 360 nm was used for analysis. The instrument was calibrated using standards of 5 gradient concentrations covering the concentrations of interest for different OVOCs in ambient air. Good linear relationships (R^2> 0.999) between the standard concentrations and responses of the instrument were obtained for the 16 analysed OVOC species. The built-in computerized programs of quality control systems such as auto-linearization and auto-calibration were used to guarantee the data quality. Detailed information about the analysis and quality control of OVOC samples was provided in Cheng et al. (2014), Cui et al. (2016) and Ling et al. (2016b). Due to the low detection rate of many OVOCs, this study only focused on formaldehyde, acetaldehyde, acetone and propionaldehyde, which had relatively high concentrations.

2.4 Model description

2.4.1 Positive matrix factorization (PMF)

PMF is a receptor model that has been extensively used for source apportionment of airborne particulate matters and VOCs (Lee et al., 1999; Brown et al., 2007). In this study, US EPA PMF 5.0 model (US EPA, 2017) was applied to identify the sources of O_3 precursors, according to Equation (1) (Paatero, 1997; Ling et al., 2014).

$$x_{ij} = \sum_{k=1}^{p} g_{ik} f_{kj} + e_{ij} \qquad \text{Equation (1)}$$

where x_{ij} is the measured concentration of *j*th species in *i*th sample, g_{ik} represents the contribution of *k*th source to *i*th sample, f_{kj} denotes the fraction of *j*th species in *k*th source, and e_{ij} is the residual for *j*th species in *i*th sample. *p* stands for the total number of independent sources (Paatero, 2000a, b).

The uncertainties of the concentrations applied to PMF were set in the same way as Polissar et al. (1998) and Reff et al. (2007). Values below or equal to the LoD were replaced by half of the LoDs and the uncertainties for these values were set as 5/6 of the corresponding LoDs. For the values greater than LoDs, the uncertainties were calculated as $[(\text{Error Fraction} \times \text{concentration})^2 + (\text{LoD})^2]^{1/2}$ where 10% was assigned as the error fraction. Missing values (mainly due to maintenance or malfunction of the instruments) were replaced by the geometric mean of the measured values and their accompanying uncertainties were set as four times the geometric mean value. More details about the settings of the uncertainty were provided in Norris et al. (2008) and Zhang et al. (2012).

The model was run for 20 times with a random seed, and tests with different number of factors were conducted. The optimum solution was finally determined based on both a good fit to the observed data and the most reasonable and interpretable results according to the knowledge on the sources of O_3 precursors in Hong Kong (Ling et al., 2011, 2014; Ou et al., 2015).

2.4.2 Observation-based model (OBM)

A photochemical box model coupled with the Master Chemical Mechanism (PBM-MCM) was used to simulate the photochemical O_3 formation on the VOC sampling days. In this study, MCM v3.2, a near explicit chemical mechanism consisting of 5,900 species and

16,500 reactions which fully describes the homogeneous gas phase reactions in the atmosphere (Jenkin et al., 1997, 2003; Saunders et al., 2003), was used. The observation data of temperature, relative humidity, O_3, SO_2, CO, NO, NO_2 and 52 C_2-C_{10} VOCs/OVOCs were input into the model. Specifically, the 52 VOCs/OVOCs included 19 alkanes, 16 alkenes, 13 aromatics and 4 OVOCs, as shown in Table S4, where the statistics of the mixing ratios of VOCs/OVOCs are also presented. Nitrous acid (HONO) was not monitored in this study. The average diurnal cycle of HONO mixing ratios measured at the same site in autumn in 2011 (Xu et al., 2015) was input into the model to roughly represent its role in O_3 formation and atmospheric radical chemistry. Due to the data limitation, the trends of HONO at TC in the three sampling campaigns were not traceable. However, the measurements at a background site in Hong Kong indicated comparable levels of HONO (p>0.1) between the autumn in 2012 and in 2018 (unpublished data). Therefore, adopting the HONO measured in 2011 as the inputs of the simulations in the three sampling campaigns was likely a plausible assumption, despite some uncertainties. The model was also tailored to the real situations in Hong Kong. Specifically, the height of the planetary boundary layer was allowed to vary from 300 m at night to 1400 m at noon. The photolysis rates were calculated according to the measured solar radiations by the Tropospheric Ultraviolet and Visible Radiation model (Madronich and Flocke, 1999; Wang et al., 2017a), with the detailed method described in Lyu et al. (2017b). In addition to the chemical processes, the exchange between the lower troposphere and free troposphere, and dry deposition were also considered in the model. The concentrations of air pollutants in the free troposphere were set according to the observations at a mountainous site in Hong Kong (Lam et al., 2013). The dry deposition rates were adopted from the previous studies (Saunders et al., 2003; Lam et al., 2013). The other physical processes were not included in the model, which might lead to insufficient description of the transport. However, since the model was constrained to the observations

283 which included the transported air pollutants, the regional transport was partially considered.
284 Besides, the observations at 07:00 on each day were used to initiate each day's modelling,
285 through which the effect of regional transport before the daytime modelling was also
286 considered. We admit that the PBM-MCM cannot perfectly reproduce the real atmospheric
287 processes. However, it performed well in describing the in-situ photochemistry in previous
288 studies (Lam et al., 2013; Ling et al., 2014; Lyu et al., 2017b; Wang et al., 2017a). Actually,
289 the deficiency of PBM-MCM in consideration of the atmospheric dynamics enabled us to
290 assess the contributions of regional transport to O_3 in Hong Kong, based on the differences
291 between the observed and simulated O_3 (Wang et al., 2017a).

292 **2.5 Simulation scenarios**

293 Two scenarios of model simulation were performed in this study, *i.e.*, Scenario A and
294 Scenario B. The scenario A simulated the O_3 photochemistry in the whole air, which was
295 constrained by the observed concentrations of all the O_3 precursors. The model simulations in
296 scenario B (including six assumed sub-scenarios) were constrained by the concentrations of
297 O_3 precursors with those contributed by individual sources being subtracted from the
298 observed concentrations. Text S1 elaborates the set-up of these scenarios. The simulated O_3
299 in scenario A was regarded as the locally produced O_3, as the observed O_3 concentrations
300 were not input to constrain the model. Bearing in mind that the regional effects cannot be
301 completely eliminated in this approach, due to the impacts of regional air on the observed
302 concentrations of O_3 precursors. The differences between the scenario A and scenarios B
303 reflected the contributions of the individual sources to the simulated O_3 production rate.

304 **3 Results and discussion**

3.1 Observation overview

Figure 2 shows the hourly mixing ratios of O_3 observed at TC in the autumns of 2007-2017 with the data on VOC sampling days being highlighted in red. It was found that the autumn O_3 increased significantly from 2007 to 2013 (p<0.01), with a rate of 0.34±0.002 ppbv yr^{-1}. This was consistent with Wang et al. (2017a) who reported an overall increase rate of autumn O_3 of 0.67±0.07 ppbv yr^{-1} at the same site for the period of 2005-2013. On one hand, the discrepancy in O_3 increasing rates might be due to the different statistics used to draw the rates, *i.e.* hourly values in this study and monthly averages in Wang et al. (2017a). On the other hand, the autumn O_3 increased substantially from 23.9±0.97 ppbv in 2005 to 30.2±0.97 ppbv in 2007, much quicker than the increase between 2007 and 2013. Without the inclusion of the period of 2005-2007 might be another reason of the less O_3 enhancement calculated here. In contrast to the increased autumn O_3 during 2007-2013, the autumn O_3 decreased obviously from 2013 to 2017 (p<0.01), at a rate of -2.27 ± 0.003 ppbv yr^{-1}, indicating a fundamental alleviation of O_3 pollution in Hong Kong in the latest 5 years. Overall, a statistically significant decreasing trend (rate = -0.44±0.001 ppbv yr^{-1}) was observed for the autumn O_3 at TC through 2007 to 2017 (p<0.05). The average O_3 on VOC sampling days in the three sampling campaigns also followed the same pattern, which increased from 32.8±2.6 ppbv in 2007 to 36.9±2.3 ppbv in 2013, while decreased to 24.4±1.9 ppbv in 2016. Further, we investigated the number of O_3 episode days in the autumns of the three VOC sampling years (see Figure S1) and identified 15 (16.5% of the autumn days, same below) and 16 (17.6%) O_3 episode days in 2007 and 2013, respectively. However, there was only 5 (5.5%) O_3 episode days in the autumn of 2016. Similarly, the O_3 episode days accounted for 12.5%, 26.3% and 5.6% of the 2007, 2013 and 2016 sampling campaigns, respectively. Therefore, the increase of O_3 from 2007 to 2013 and the decrease in the following years could be represented by O_3 observed in the three sampling periods.

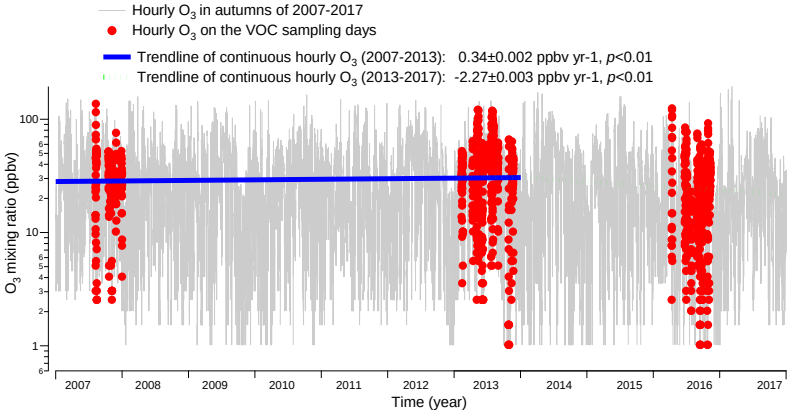

330

331 Figure 2. Long-term trends of the observed O_3 at TC from 2007 to 2017. Hourly O_3 values on
332 the VOC sampling days in the autumns of 2007, 2013 and 2016 are marked in red.

333

334 Table 1 and Table S5 present the observed O_3, CO, NO, NO_2, SO_2 and TVOCs, as well as the
335 meteorological conditions averaged on the VOC sampling days in 2007, 2013 and 2016,
336 respectively. From 2007 to 2013, the TVOCs decreased by nearly a half, which was expected
337 to result in the reduction of O_3 in view of the VOC-limited regime of O_3 formation at TC
338 (Cheng et al., 2010; Wang et al., 2017a). However, the increases of CO and the notable
339 decrease of NO in 2013 could enhance the O_3 production. The higher O_3 in 2013 indicated
340 that this effect overrode the reduction of TVOCs in influencing the O_3 production. In
341 particular, the decrease of NO meant the reduced NO titration to O_3, which has been
342 recognized as a primary reason of O_3 increase in VOC-limited regime (Chou et al., 2006;
343 Wang et al., 2018b). From 2013 to 2016, the decrease of O_3 was accompanied by the
344 reductions of TVOCs and NO_2, though CO remained increasing at the same time. NO_2, as a
345 direct source of O_3 through photolysis, plays important role in modulating the O_3 variation.
346 Though the causes of NO_2 reduction are unknown to us, it might be one of the critical factors
347 contributing to the decline of O_3 in Hong Kong in recent years. On the contrary, the increase

of CO was also confirmed by the continuous monitoring data at TC, with a rate of 33.9 ± 0.7 ppbv yr^{-1} between 2013 and 2016. In fact, the consistent increasing trend ($p<0.05$) was also observed at the roadside sites in Hong Kong (not shown here). While the causes of CO increase in Hong Kong may be complicated, the increased vehicle emission is a plausible explanation. Studies (Johnson, 2008; Yao et al., 2008) revealed that while the new engine technologies performed well in reducing NO_x emission, they might lead to the increased emission of CO, with the application of lower air-to-fuel ratio and engine temperature.

In addition, studies have confirmed that continental anticyclones and tropical cyclones are conducive to severe O_3 pollution in Hong Kong, because these synoptic systems are often accompanied with northerly winds, high temperature, strong solar radiation, and relatively high pressure in Hong Kong (Ding et al., 2004; Huang et al., 2005; Jiang et al., 2015). Table S6 summarizes number of O_3 episode days with tropical cyclone, continental anticyclone and low pressure trough in the autumns of 2007, 2013 and 2016. In autumn 2007, 8, 8 and 1 O_3 episode day(s) were found to be related to the tropical cyclone, continental anticyclone and low-pressure trough, respectively, with 2 O_3 episode days under the combined influence of tropical cyclone and continental anticyclone. There were also 11 and 5 O_3 episode days in association with tropical cyclone and continental anticyclone in autumn 2013, respectively (Wang et al., 2018b). However, 4 of the 5 episode days found in autumn 2016 were associated with tropical cyclone, with the other one relative to low-pressure trough. Therefore, the lower O_3 and less O_3 episode days in 2016 were also benefited from the meteorological conditions.

Table 1. Mixing ratios of the measured trace gases and TVOCs averaged on the selective 45 VOC sampling days in 2007, 2013 and 2016.

	2007	**2013**	**2016**

Unit: ppbv	Mean ±95% C.I.	Max.	Mean ±95% C.I.	Max.	Mean ±95% C.I.	Max.
O_3	32.8±2.6	137.0	36.9±2.2	121.2	24.4±1.9	124.9
CO	456.3±19.8	847.0	585.0±11.9	1047.9	691.8±9.5	1074.7
NO	17.2±3.2	124.7	10.9±1.3	98.6	11.3±1.4	94.6
NO_2	27.7±2.1	69.6	31.5±1.4	80.8	22.0±1.1	103.2
SO_2	6.9±0.4	21.8	7.0±0.2	18.0	3.0±0.1	10.7
TVOCs	49.7±4.4	111.1	25.1±1.4	68.0	21.1±1.4	71.9

3.2 Model simulation of O_3

3.2.1 Model validation

Figure 3 compares the simulated O_3 in scenario A and the observed O_3 on the VOC sampling days. Overall, both the magnitudes and the temporal patterns of the observed O_3 were reasonably reproduced, though the mean of the simulated O_3 (30.0±1.7 ppbv) was slightly lower than the observed average (38.1±2.0 ppbv). To quantitatively evaluate the model performance, the index of agreement (IOA) was used to examine the goodness of fit between simulated and observed O_3. Within the range of 0-1, higher IOA represents better agreement between the simulated and observed values (Willmott, 1982). In this study, the overall IOA for the three sampling periods was 0.68, within the range of IOA (0.67-0.89) accepted by the previous studies (Wang et al., 2015; Lyu et al., 2015, 2016a, c; Wang et al., 2017a, 2018a). Good correlations (R^2=0.61) were also shown between the simulated and observed hourly O_3. Bearing in mind the deficiencies of the box model in describing the atmospheric dynamics, we believed that the modelling results were acceptable, but special attention and explanation to the discrepancies between the simulated and observed O_3 was needed.

It was found that the discrepancies were most likely caused by the transport processes, *i.e.*, vertical and horizontal transport, which were not fully represented in the PBM-MCM model (George et al., 2013; Lakey et al., 2015; Wang et al., 2017a). For example, the simulated O_3 (maximum: 122.6 ppbv) was much higher than the observed O_3 (maximum: 44.3 ppbv) on November 16, 2007, when the strong southeast winds (wind direction: 90°-180°) with the highest wind speed of 5.3 m s^{-1} prevailed in Hong Kong. The south sector winds from SCS might dilute the locally produced O_3 and the O_3 precursors/intermediates (such as the radicals) which were not constrained by the observations. The same circumstances were also observed on October 27, November 17, 2007 and September 11-12, November 20, 2013, with southeast winds dominated (74.4%) during the daytime (Figure 3). For those days with the simulated O_3 lower than the observed O_3, *i.e.* October 3, 22-25, 2013 and November 6, 2016, 69.3% of the winds during the daytime came from the north (wind directions: 0-90° and 270°-360°), which might transport the air masses laden with O_3 and/or O_3 precursors/intermediates not constrained to the observations from inland PRD to the sampling site. The observed O_3 mixing ratios are plotted against the wind fields in Figure S2. It is obvious that O_3 were higher under the north winds, while lower in the south wind sectors, confirming the effects of dilution and regional transport of the south and north winds on O_3 pollution in Hong Kong, respectively.

Atmos. Chem. Phys. Discuss., https://doi.org/10.5194/acp-2018-1148
Manuscript under review for journal Atmos. Chem. Phys.
Discussion started: 11 December 2018

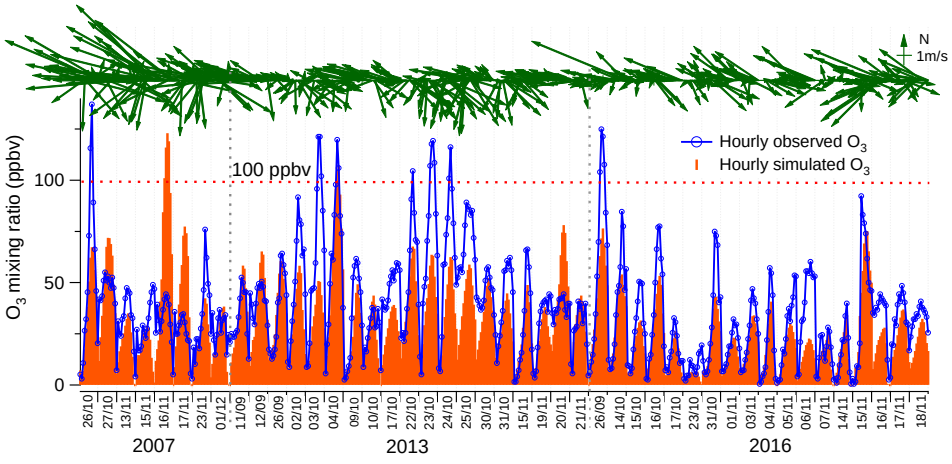

404

405 Figure 3. Hourly mixing ratio of the simulated and observed O_3 at TC during the VOC
406 sampling periods in 2007, 2013 and 2016. The arrows represent the hourly wind sectors
407 monitored at the sampling site.

408 **3.2.2 Inter-annual variations of the locally produced and regional transported O_3**

409 As discussed in section 2.5, the simulated O_3 in scenario A could be regarded as the locally
410 produced O_3. Therefore, the differences between the observed O_3 and O_3 simulated in
411 scenario A were treated as the regionally transported O_3 (Wang et al., 2017a). It is
412 noteworthy that some negative values were generated with this method, corresponding to the
413 dilution of the south winds to the locally produced O_3 as elaborated in section 3.2.1. Figure 4
414 shows the hourly mixing ratios of the observed, local and regional O_3 at TC in daytime hours
415 (07:00-19:00 LT) of the three sampling campaigns. Overall, the observed O_3 was mainly
416 (78.3±2.4%) contributed by the local photochemical production, with regional transport only
417 accounting for 21.7±2.4% of the observed daily maximum O_3. However, regional transport
418 was responsible for as high as 40.9±39.2% of the observed daily maximum O_3 in Hong Kong
419 on the O_3 episode days when northerly winds prevailed, indicating the heavy O_3 burden
420 superimposed by regional air masses from PRD. From 2007 to 2013, both the observed and

simulated locally-produced O_3 remained statistically unchanged (p>0.1), in contrast to the increase of regional O_3 at a rate of 1.62±0.39 ppbv yr^{-1} (p<0.05), similar to that (1.09±0.21ppbv yr^{-1}) reported by Wang et al. (2017a) in the autumns of 2005-2013. However, the decease of the locally produced O_3 in the same period as that simulated by Wang et al. (2017a) was not seen here according to the simulated O_3 in the 2007 and 2013 sampling campaigns. This discrepancy was likely caused by the limited samples in this study, no OVOCs considered in Wang et al. (2017a) and/or the inexactly same study periods between the two studies. Instead, we found that the locally produced O_3 showed a significant decline at a rate of -4.35±0.10 ppbv yr^{-1} during 2013-2016 (p<0.05), when the regionally transported O_3 also decreased (10.9±2.0 and 8.9±1.8 ppbv in the 2013 and 2016 sampling campaign, respectively). As a result, the increase of the observed O_3 from 2007 to 2013 was reversed by the decrease between 2013 and 2016, leading to an overall decreasing trend of the observed O_3 during 2007-2016 (rate = -0.54±0.15 ppbv yr^{-1}, p<0.05).

Atmos. Chem. Phys. Discuss., https://doi.org/10.5194/acp-2018-1148
Manuscript under review for journal Atmos. Chem. Phys.
Discussion started: 11 December 2018

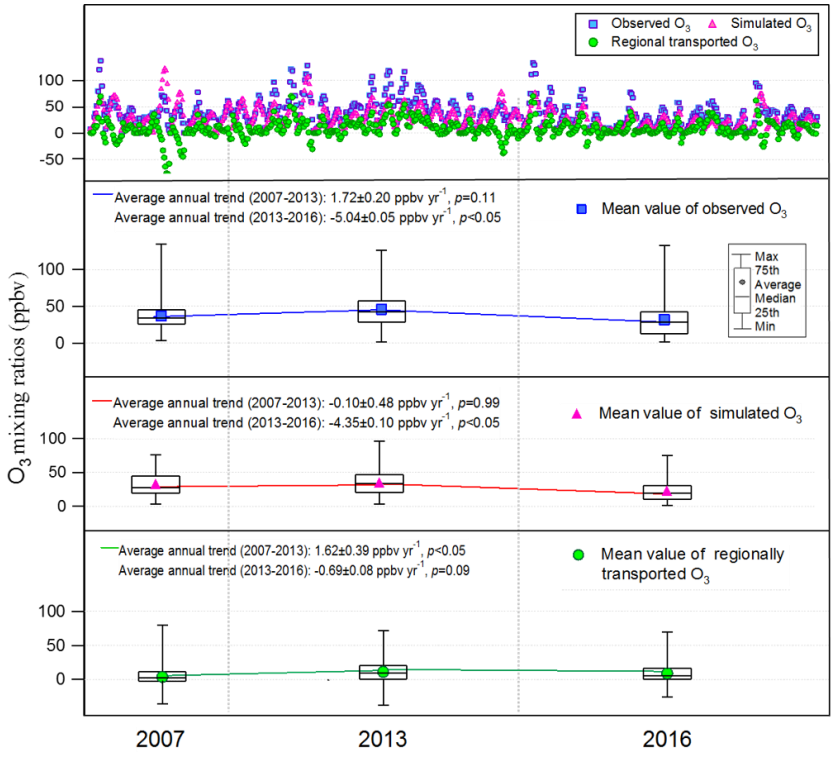

Figure 4. Hourly values (first panel) and the throughout-campaign statistical results (second to fourth panels) of the observed, simulated (locally-produced) and regional O_3 mixing ratios in daytime hours (07:00 – 19:00 LT) in the three sampling campaigns.

The significant alleviation of O_3 pollution in Hong Kong from 2013 to 2016 might be related to the measures taken to control the emissions of O_3 precursors in Hong Kong and in mainland China. The effectiveness of the actions launched by Hong Kong government in O_3 abatement was fully demonstrated in previous studies (Xue et al., 2014a; Lyu et al., 2017a; Wang et al., 2017a), and would be further evaluated in this study (section 3.4). Besides, the emission controls in mainland China might contribute to the decrease of O_3 in this period. For example, the China's NO_x emissions for the first time showed a decreasing trend from 2013, benefited from the implementation of the China's Clean Air Action Plan (Zheng et al., 2018).

447 Furthermore, we looked into the monthly average O_3 observed at the 12 air quality
448 monitoring stations across the inland PRD, including three regional monitoring stations, *i.e.*
449 Tianhu, Wanqingsha and Jinguowan, and nine urban monitoring stations, *i.e.* Xiapu, Jinjuzui,
450 Donghu, Tangjia, Liyuan, Huijingcheng, Zimaling, Luhu and Chengzhong
451 (https://www.epd.gov.hk /epd/sc_chi/resources_pub/publications/m_report.html). As shown
452 in Figure 5, O_3 at these stations remained relatively stable (p=0.99) during 2006-2013, which
453 however showed a contrastively decreasing trend at a rate of -1.73±0.08 ppbv yr^{-1} from 2013
454 to 2016. This corroborated our modelling results that the regional contribution to O_3 in Hong
455 Kong ceased increasing or even began to decrease since 2013. Though the substantial
456 decrease of NO_x was a plausible reason for the alleviated regional O_3 pollution, analyses of
457 the causes are out of the scope of this study. In addition to the reduced local formation and
458 regional transport of O_3, the more favourable meteorological conditions in 2016 might be
459 another reason of the O_3 decrease, as discussed in section 3.1.

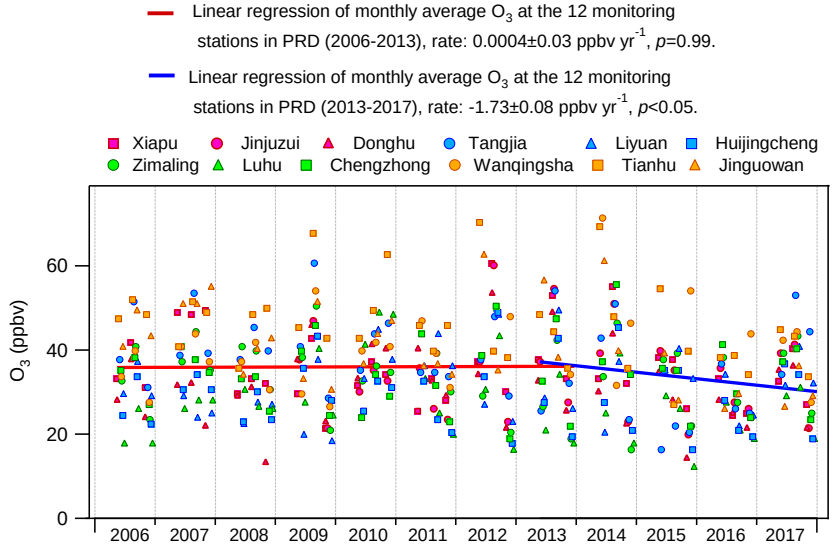

460

461 Figure 5. Trends of the observed monthly average O_3 at the 12 air quality monitoring stations
462 in inland PRD.

Atmos. Chem. Phys. Discuss., https://doi.org/10.5194/acp-2018-1148
Manuscript under review for journal Atmos. Chem. Phys.
Discussion started: 11 December 2018

3.3 Local production and destruction pathways of O_3 and OH radical

3.3.1 In-situ net O_3 production

Figure 6 shows the average diurnal profiles of the simulated O_3 production and destruction pathways during the three sampling campaigns. Also shown are the average diurnal cycles of the simulated O_3. The shift of the peaks between the net O_3 production rate and the simulated O_3 was due to the accumulation of the newly generated O_3 over time in the model, which was also true in the real situations. The reactions between NO_2 and O_3, leading to the formation of NO_3 and N_2O_5, in addition to dry deposition and aloft exchange, were the main depletions of the simulated O_3 in the late afternoon. Consistent with previous studies (Kanaya et al., 2009; Liu et al., 2012; Xue et al., 2014b), these pathways were not included in the calculation of the net O_3 production rate, because we mainly focused on the photochemical processes in the hours when O_3 was accumulated. It was found that the reaction between HO_2 with NO dominated the O_3 production rates in all the cases, with an average rate of 3.0±0.6 ppbv h^{-1} (72.6±15.1%, percentage of the total O_3 production rate, same below), 2.1±0.3 ppbv h^{-1} (77.8±9.9%) and 1.1±0.2 ppbv h^{-1} (80.7±11.6%) in the 2007, 2013 and 2016 sampling campaigns, respectively. In addition, the sum of the reaction rates between RO_2 radicals and NO contributed 1.1±0.2 ppbv h^{-1} (27.4±5.3%), 0.6±0.1 ppbv h^{-1} (22.2±3.0%) and 0.3±0.04 ppbv h^{-1} (19.3±3.1%) to the O_3 production rate in 2007, 2013 and 2016, respectively. The formation of HNO_3 though the reaction between OH and NO_2 served as the main scavenger pathway of O_3, as NO_2 would be photolyzed and produce O_3 otherwise. On average, O_3 was consumed in this way at a rate of -1.0±0.1 ppbv h^{-1} (82.6±12.0%, percentage of the total O_3 destruction rate, same below), -0.9±0.1 ppbv h^{-1} (83.1±7.7%) and -0.5±0.05 ppbv h^{-1} (83.4±8.4%) in 2007, 2013 and 2016, respectively. The photolysis of O_3 was the second contributor to O_3 destruction, with an average contribution of -0.09±0.01 ppbv h^{-1} (10.5±1.1%) for the three sampling periods. Besides, the ozonolysis of unsaturated

Atmos. Chem. Phys. Discuss., https://doi.org/10.5194/acp-2018-1148
Manuscript under review for journal Atmos. Chem. Phys.
Discussion started: 11 December 2018

488 VOCs and the reactions between O_3 and radicals (OH and HO_2) were responsible for 4.1±0.5%
489 and 2.3±0.3% of the total destruction rate of the locally produced O_3, respectively.
490 Overall, the net local O_3 production rate decreased from 3.0±0.7 ppbv h^{-1} in 2007, to
491 1.6±0.3 ppbv h^{-1} in 2013, till 0.8±0.2 ppbv h^{-1} in 2016, corresponding to the decline of the
492 locally produced O_3 through 2007 to 2016 (Section 3.2.2).

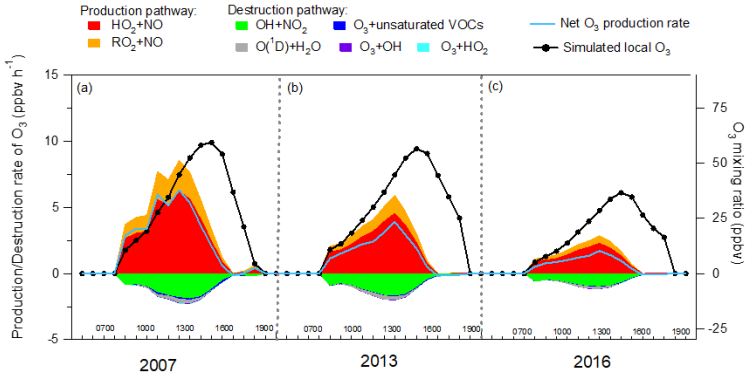

493

494 Figure 6. Average diurnal profiles of the local O_3 production and destruction rates in the
495 sampling campaigns of (a) 2007, (b) 2013 and (c) 2016.

496 **3.3.2 Recycling of OH radical**

497 As one of the most important radicals in the atmosphere, OH initiates the oxidation of VOCs,
498 leading to O_3 formation. Figure 7 presents the average diurnal profiles of the simulated OH
499 and the formation and loss pathways dominating the recycling of OH during the three
500 sampling periods. According to the simulation by PBM-MCM model, the average OH
501 concentration was (1.4±0.3) × 10^6 molecules cm^{-3} in the 2007 sampling campaign, which
502 significantly decreased to (1.3±0.2) × 10^6 molecules cm^{-3} in the 2013 sampling campaign
503 (p<0.05) and further decreased to (0.9±0.1) × 10^6 molecules cm^{-3} in 2016 (p<0.05).

504 As expected, the formation and loss rates of OH were basically balanced in all the cases. OH
505 was mainly formed from the reaction of HO_2+NO, which accounted for 58.2±2.3% of the

506 total OH production rate over the three sampling campaigns. The photolysis of HONO and
507 O_3 made comparable but much lower contributions (19.2±1.4% and 19.3±2.9%, respectively)
508 to the production of OH, with the rest attributable to the ozonolysis of unsaturated VOCs
509 (2.8±0.2%) and the photolysis of H_2O_2 (0.2±0.01%). On the contrary, OH was mainly
510 depleted by the reactions with NO_2 (39.2±1.1%), VOCs (25.3±0.9%), CO (21.0±0.6%) and
511 NO (14.1±1.1%).

512 Consistent with the variations of the local O_3 production, both the local formation and loss
513 rates of OH decreased through 2007 to 2016 (p<0.05), with much more obvious reductions in
514 the later phase (2013-2016). On one hand, the continuous reduction of VOCs resulted in
515 lower HO_2 and RO_2 concentrations (Figure S3), hence the lower production rate of OH
516 through the reaction of HO_2+NO. At the same time, the destruction rates of OH also
517 decreased due to the reductions of OH and the O_3 precursors, except for CO (Figure 7 and
518 Table 1). The decreases of the OH production and destruction rates indicated that the
519 propagation of the reaction cycles, namely the recycling of OH, became slower from 2007 to
520 2016. This also explained why the locally produced O_3 decreased in these ten years, since O_3
521 is formed with the consumption and recycling of OH radical.

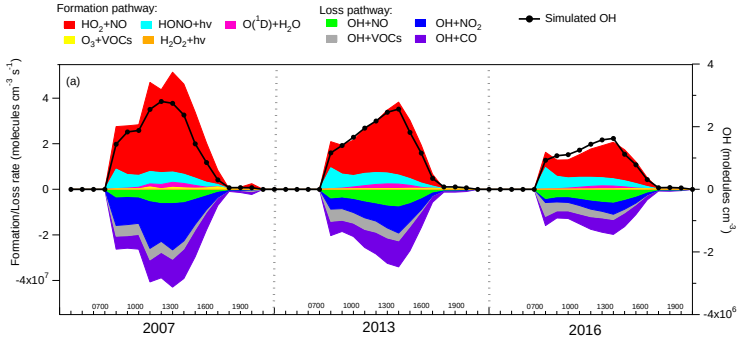

522

523 Figure 7. Average diurnal cycles of the OH formation and loss rates during the sampling
524 periods in (a) 2007, (b) 2013 and (c) 2016.

3.4 Source contributions to the production of O_3 and radicals

3.4.1 Source apportionment

To resolve the sources of O_3 precursors, 27 species, including CO, NO, NO_2, 12 alkanes, 4 alkenes and 8 aromatics, were applied to PMF for source apportionment. These species were either of high abundances or typical tracers of VOC sources in Hong Kong. Source apportionment was conducted for a total of 414 samples covering the three sampling periods, so that the uncertainty of the source apportionment results could be reduced, compared to separate source apportionments for each of the three sampling periods. Figure 8 shows the average profiles of the six sources resolved by PMF. The modelling errors were estimated with the bootstrap method integrated in PMF (Brown et al., 2015).

Factor 1 was assigned as the combination of LPG usage and gasoline evaporation, in view of the high loadings of C_2-C_5 hydrocarbons. Specifically, propane and *i*-/*n*-butanes are the main components of LPG in Hong Kong, and gasoline evaporation generally contains large quantities of *i*-/*n*-pentanes, in particularly *i*-pentane (Guo et al., 2013; Lyu et al., 2017a). Factor 2 was characterized by moderate to high percentages of *i*-/*n*-pentanes and TEX (toluene, ethylbenzene and xylenes). These species are commonly seen in gasoline exhausts. Therefore, we defined this factor as gasoline exhausts. Both the third and fourth factors indicated solvent-related emissions. While Factor 3 likely represented household solvent usage, due to the dominance of hexane and hexane isomer (3-methylpentane) (Ling and Guo, 2014; Ou et al., 2015), Factor 4 was more related to emissions from coatings and paints, in view of the dominance of the aromatics (Ling and Guo, 2014). Factor 5 was distinguished by the high concentrations of ethane, ethene, ethyne and benzene, together with the relatively heavy (C_7-C_{10}) alkanes, which are typical species in diesel exhausts (Schauer et al., 1999; Kashdan et al., 2008; Sahoo et al., 2011). Therefore, this factor was designated as diesel

549 exhausts. The last factor denoted for biogenic emissions (BVOCs), due to the exclusive
550 dominance of isoprene (Guenther, 2006).

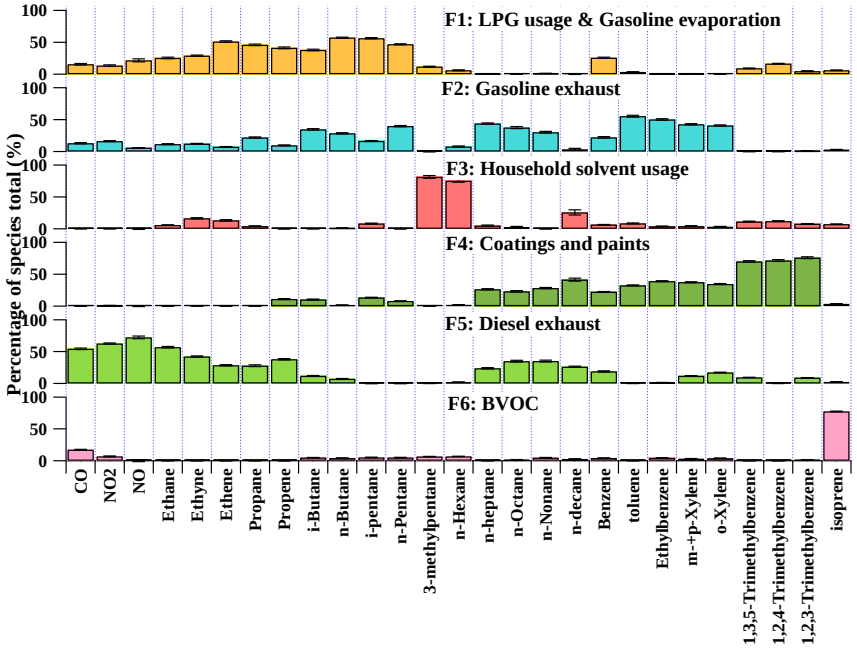

551

552 Figure 8. Average profiles of the O_3 precursors sources at TC in the three sampling
553 campaigns. The uncertainties were estimated with the bootstrap method in PMF.

554

555 Figure S4 presents the total mixing ratio of VOCs emitted from each individual source
556 extracted from PMF during the three sampling periods in Hong Kong. The VOC emissions
557 from LPG usage and gasoline evaporation decreased significantly (p<0.05) at a rate of -
558 2.61±0.03 ppbv yr^{-1} from 2007 to 2016. However, the VOCs in association with gasoline
559 exhausts experienced an increase (rate = 1.32±0.02 ppbv yr^{-1}, p<0.05) in these years,
560 indicating that the reduction of VOC emissions from LPG usage and gasoline evaporation
561 was not attributable to the change in emissions of gasoline-fuelled vehicles. Insight into the
562 mixing ratios of propane and *i*-/*n*-butanes (LPG tracers) in this source revealed a significant

563 decline from 3.51±0.52 ppbv in the 2007 sampling campaign to 1.27±0.11 ppbv in the 2016
564 sampling campaign. Therefore, the reduction of VOC emissions from LPG usage was most
565 likely the reason of the decrease of VOCs allocated to the source of LPG usage and gasoline
566 evaporation. In fact, it was confirmed by our previous studies (Lyu et al., 2016b; Yao et al.,
567 2019) that the replacement of catalytic converters on LPG-fuelled vehicles during September
568 2013-May 2014 effectively reduced the VOC emissions from LPG-fuelled vehicles in Hong
569 Kong. In addition, the variations in LPG usage in inland PRD, where LPG was extensively
570 used as vehicular and domestic fuels (Liu et al., 2008), might also contribute to the emission
571 reduction of VOCs, in view of the decrease of LPG tracers in this source from 2007
572 (3.51±0.52 ppbv) to 2013 (2.04±0.27 ppbv), when no control was performed against LPG
573 fuelled vehicle emissions in Hong Kong. The VOCs emitted from solvent usage (including
574 the household solvent, coatings and paints) also decreased significantly (p<0.05) from 2007
575 to 2016, likely benefiting from the actions taken to restrict the VOC contents in solvent
576 products starting from 2007 (phase I) and 2010 (phase II) in Hong Kong (Lyu et al., 2017a).
577 VOCs attributable to diesel exhausts decreased (p<0.05) from the 2007 (2.6±0.3 ppbv) to
578 2013 sampling campaign (2.0±0.2 ppbv), which however were unchanged between 2013 and
579 2016 (2.2±0.2 ppbv). In fact, a subsidy program has been implemented in Hong Kong since
580 2007 to progressively eliminate the pre-Euro IV diesel vehicles or to upgrade their emission
581 standards to Euro IV (HKEPD, 2017b), and the effectiveness of this program in VOC
582 reductions till 2013 was confirmed by Lyu et al. (2017a) with the online measurement data at
583 the same site. However, while the phase III of this program (2014-2019) is still ongoing, the
584 VOCs emitted from diesel vehicles remained stable between the 2013 and 2016 sampling
585 campaigns. This undesirable result might be due to the fact that the actions were mainly
586 targeted at the pre-Euro, Euro I and Euro II diesel vehicles before 2013, whereas the phase III
587 of the program initiated in 2014 focused on the Euro III vehicles (HKEPD, 2017b, 2018).

588 Since the former were vehicles with higher emissions, it is not unreasonable that reduction of
589 VOCs was more discernible between 2007 and 2013. Further, the effectiveness of the phase
590 III program might be somewhat offset by the wearing-out of the pre-existing vehicles and the
591 increase of diesel vehicle populations (Competition Commission, 2017). Further evaluation
592 with more data in a longer period is recommended. At last, the increase of BVOCs from 2007
593 to 2013 but comparable levels between 2013 and 2016 seemed to be related to the lower
594 (p<0.05) temperature in the 2007 sampling campaign (Table S5).

595 **3.4.2 Source contributions to O_3 production**

596 Figure 9 presents the contributions of VOCs emitted from individual sources to the
597 production and destruction rates of O_3, as well as the simulated contributions to the O_3
598 mixing ratios. NO_x was not included in these analyses, because of its relatively high
599 uncertainties in source apportionment results due to the short lifetimes. Consistent with the
600 O_3 production and destruction in the whole air, the pathway of HO_2+NO dominated over the
601 reactions between RO_2 and NO in O_3 production for all the individual sources. The
602 destruction of O_3 was mainly driven by NO_2 reacting with OH. For the net O_3 production rate,
603 VOCs attributable to the coatings and paints made the largest contribution (0.38±0.05 ppbv h^{-1}),
604 followed by gasoline exhausts (0.22±0.03ppbv h^{-1}), LPG and gasoline evaporation
605 (0.21±0.03ppbv h^{-1}), BVOCs (0.19±0.03ppbv h^{-1}), household solvent usage (0.15±0.04 ppbv
606 h^{-1}) and diesel exhausts (0.13±0.01ppbv h^{-1}). Despite some peak shifts for the reasons
607 illustrated in section 3.3.1, the O_3 mixing ratios elevated by the individual sources followed
608 the same pattern as the net O_3 production rates, with the highest O_3 enhancement (1.92±0.21
609 ppbv) by the source of coatings and paints and the lowest increase by household solvent
610 usage (0.86±0.06 ppbv) and diesel exhausts (0.83±0.06 ppbv). The contributions of source-
611 specific VOCs to O_3 production, particularly the importance of solvent usage in O_3 formation
612 in Hong Kong, were generally in line with previous studies (Ling and Guo, 2014; Ou et al.,

613 2015). This was actually expected according to the reactivity of major VOCs in each source.
614 For example, the TEX in the source of coatings and paints (Figure 8) have been identified to
615 be of high O_3 formation potentials (Lau et al., 2010; Ling et al., 2011, 2013). However, the
616 PBM-MCM model simulations enabled us to quantitatively evaluate the contributions of
617 VOC sources to O_3 production rates.

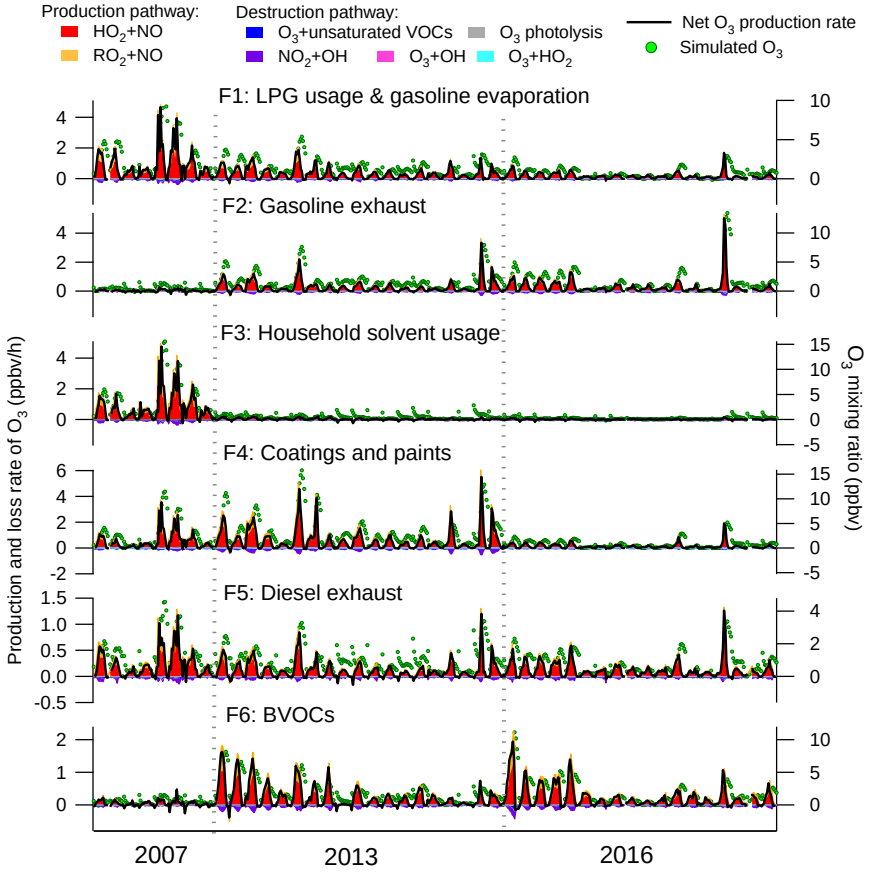

618

619 Figure 9. Contributions of VOCs in individual sources to the production and destruction rates
620 of O_3 and to the O_3 mixing ratios in the three sampling campaigns.

621 From a historical perspective, we found that the contribution of LPG usage and gasoline
622 evaporation to O_3 production significantly decreased (p<0.05) from 2007 to 2016 sampling

campaign (2007: 0.51±0.11 ppbv h^{-1}; 2013: 0.20±0.03 ppbv h^{-1}; 2016: 0.10±0.02 ppbv h^{-1}), which coincided with the variations of VOCs emitted from LPG-fuelled vehicles as discussed above. Gasoline exhaust contributed much less (p<0.05) to the net O_3 production rate in 2007 (0.02±0.01ppbv h^{-1}), than those in 2013 (0.26±0.05ppbv h^{-1}) and 2016 (0.27±0.07ppbv h^{-1}), in line with the variations of VOCs emitted from this source. The reductions of VOC emissions from solvents also resulted in the consistent decrease of the net O_3 production rate from 1.22±0.17 ppbv h^{-1} in the 2007 to 0.14±0.05 ppbv h^{-1} in the 2016 sampling campaign. The O_3 production rates contributed by VOCs in diesel exhausts were reduced from 2007 (0.21±0.05 ppbv h^{-1}) to 2013 (0.11±0.02 ppbv h^{-1}) and remained unchanged thereafter (2016: 0.11±0.02 ppbv/h). The O_3 production rate traceable to BVOCs showed a significant increase from 2007 (0.04±0.02 ppbv h^{-1}) to 2016 (0.22±0.04 ppbv h^{-1}), since the mixing ratios of BVOCs significantly increased (p<0.05) in these years. It is noteworthy that the changes in meteorological conditions in these three sampling campaigns might also partially account for the variations in the source contributions to O_3 production. For example, the 2013 sampling campaign was characterized by the relatively higher temperature and lowest relative humidity among the three sampling periods, which favoured O_3 formation in 2013 (Table S5). Besides, due to limited samples in this study, we recommend further assessments with more data in longer periods to be carried out in future study.

4 Conclusions

Photochemical pollution with high and increasing concentrations of O_3 has been an important environmental issue in South China. With the observation data of O_3 and its precursors at a suburban site in Hong Kong, downwind of South China, this study analysed the inter-annual variations of O_3 and its photochemistry, as well as the contributions of VOC sources to the local O_3 production rates in 2007, 2013 and 2016. To our knowledge, this is the first time that a substantial alleviation of O_3 pollution in this region was identified between 2013 and 2016,

in contrast to the repeatedly confirmed O_3 increase before 2013. In addition to the changes in meteorological conditions among the three sampling campaigns, the termination of the rise in regionally transported O_3 and the decrease of the local O_3 production rate contributed to the decline of O_3 in the later period. The emission reductions (particularly for NO_x) in mainland China starting from 2013, the year when the China's Clean Air Act Plan was launched, might more or less play a role in ceasing the increase of regional O_3. In Hong Kong, the replacement of catalytic converters and the constraints of VOC contents in solvent products led to the reductions of VOC emissions from LPG-fuelled vehicles and solvent usage, respectively. As a result, the local O_3 production rate and the recycling rate of OH radical decreased substantially from 2013 to 2016. Though the variations in meteorological conditions and the limited sample size might somewhat introduce uncertainties to the conclusions drawn from the present study, it is plausible that the local and regional interventions were effective on the control of O_3 pollution in Hong Kong. Nevertheless, studies with more data in longer periods should be conducted, not only in Hong Kong but also in mainland China where O_3 is still increasing in most of the territories.

Author contribution

Hai Guo and Fei Jiang initiated and designed the experiments, and Xufei Liu and Xiaopu Lyu carried them out. Xiaopu Lyu and Yu Wang developed the model code and performed the simulations. Xufei Liu and Xiaopu Lyu prepared the manuscript and Hai Guo finalized the manuscript with contributions from all co-authors.

Acknowledgements

This study was supported by the National Key R&D Program of China via grant No. 2017YFC0212001, Research Grants Council of the Hong Kong Special Administrative Region Government via grants PolyU 152052/14E, PolyU 152052/16E and CRF/C5004-15E,

672 the Public Policy Research Funding Scheme from Policy Innovation and Co-ordination
673 Office of the Hong Kong Special Administrative Region Government (Project Number:
674 2017.A6.094.17D), and the Hong Kong Polytechnic University Ph.D. scholarships via
675 research project #RUDC.

676 **References**

677 Ashmore, M. R.: Assessing the future global impacts of ozone on vegetation, Plant. Cell.
678 Environ., 28, 949-964, 2005.
679 Bell, M. L., McDermott, A., Zeger, S. L., Samet, J. M., and Dominici, F.: Ozone and short-
680 term mortality in 95 US urban communities, 1987-2000, JAMA, 292, 2372-2378, 2004.
681 Brown, S. G., Frankel, A., and Hafner, H. R.: Source apportionment of VOCs in the Los
682 Angeles area using positive matrix factorization, Atmos. Environ., 41, 227-237, 2007.
683 Brown, S. G., Eberly, S., Paatero, P., and Norris, G. A.: Methods for estimating uncertainty in
684 PMF solutions, Sci. Total Environ., 518, 626-635, 2015.
685 Census and Statistics Department (CSD), 2011 Population Census in Hong Kong, available at:
686 https://www.census2011.gov.hk/en/constituency-area-i.html (last access: 25 October 2018),
687 2011.
688 Census and Statistics Department (CSD), District profile for 2016 Population Census in Hong
689 Kong, available at: https://www.bycensus2016.gov.hk/en/bc-dp.html (last access: 25 October
690 2018), 2018.
691 Cheng, H. R., Guo, H., Wang, X. M., Saunders, S. M., Lam, S. H. M., Jiang, F., Wang, T. J.,
692 Ding, A. J., Lee, S. C., and Ho, K. F.: On the relationship between ozone and its precursors in
693 the Pearl River Delta: application of an observation-based model (OBM), Environ. Sci. Pollut.
694 Res., 17, 547-560, 2010.

695 Cheng, H. R., Saunders, S. M., Guo, H., Louie, P. K. K., and Jiang, F.: Photochemical
696 trajectory modeling of ozone concentrations in Hong Kong, Environ. Pollut, 180, 101-110,
697 2013.
698 Cheng, Y., Lee, S. C., Huang, Y., Ho, K. F., Ho, S. S. H., Yau, P. S., Louie, P. K. K., and
699 Zhang, R. J.: Diurnal and seasonal trends of carbonyl compounds in roadside, urban, and
700 suburban environment of Hong Kong, Atmos. Environ., 89, 43-51, 2014.
701 Chou, C. C. K, Liu, S. C., Lin, C. Y., Shiu, C. J., and Chang, K. H.: The trend of surface
702 ozone in Taipei, Taiwan, and its causes: Implications for ozone control strategies, Atmos.
703 Environ., 40, 3898-3908, 2006.
704 Colman, J. J., Swanson, A. L., Meinardi, S., Sive, B. C., Blake, D. R., and Rowland, F. S.:
705 Description of the analysis of a wide range of volatile organic compounds in whole air
706 samples collected during PEM-Tropics A and B, Anal. Chem., 73, 3723-3731, 2001.
707 Competition Commission: Report on Study into Hong Kong's Auto-fuel Market, available at:
708 https://www.compcomm.hk/en/media/press/files/Full_Report_Auto_fuel_Market_Study_Rep
709 ort_Eng.pdf (last access: 25 October 2018), 2017.
710 Cui, J., Pandey Deolal, S., Sprenger, M., Henne, S., Staehelin, J., Steinbacher, M., and
711 Nédélec, P.: Free tropospheric ozone changes over Europe as observed at Jungfraujoch
712 (1990–2008): An analysis based on backward trajectories, J. Geophys. Res. Atmos., 116,
713 D10304, https://doi.org/10.1029/2010JD015154, 2011.
714 Cui, L., Zhang, Z., Huang, Y., Lee, S. C., Blake, D. R., Ho, K. F., Wang, B., Gao, Y., Wang,
715 X. M., and Louie, P. K. K. Measuring OVOCs and VOCs by PTR-MS in an urban roadside
716 microenvironment of Hong Kong: relative humidity and temperature dependence, and field
717 inter-comparisons, Atmos. Meas. Tech., 9, 5763-5779, 2016.
718 Derwent, R. G., Manning, A. J., Simmonds, P. G., Spain, T. G., and O'Doherty, S.: Analysis
719 and interpretation of 25 years of ozone observations at the Mace Head Atmospheric Research

720 Station on the Atlantic Ocean coast of Ireland from 1987 to 2012, Atmos. Environ., 80, 361-
721 368, 2013.
722 Ding, A. J., Wang, T., Zhao, M., Wang, T. J., and Li, Z. K.: Simulation of sea-land breezes
723 and a discussion of their implications on the transport of air pollution during a multi-day
724 ozone episode in the Pearl River Delta of China, Atmos. Environ., 38, 6737-6750, 2004.
725 Ding, A.J., Wang, T., Thouret, V., Cammas, J., and Nédélec, P.: Tropospheric ozone
726 climatology over Beijing: analysis of aircraft data from the MOZAIC program, Atmos. Chem.
727 Phys., 8, 1-13, 2008.
728 Dongguan Environment Protection Department (DGEPD), Clean air action plan in Pearl
729 River Delta region, Phase II (2013-2015), available at: http://dgepb.dg.gov.cn
730 /publicfiles///business/htmlfiles/dgepb/cmsmedia/document/doc172679.pdf (last access: 25
731 October 2018), 2013.
732 Guenther, A., Karl, T., Harley, P., Wiedinmyer, C., Palmer, P.I., and Geron, C.: Estimates of
733 global terrestrial isoprene emissions using MEGAN (Model of Emissions of Gases and
734 Aerosols from Nature), Atmos. Chem. Phys., 6, 3181-3210, 2006.
735 George, I. J., Matthews, P. S. J., Whalley, L. K., Brooks, B., Goddard, A., Baeza-Romero, M.
736 T., and Heard, D. E.: Measurements of uptake coefficients for heterogeneous loss of HO_2
737 onto submicron inorganic salt aerosols, Phys. Chem. Chem. Phys., 15, 12829-12845, 2013.
738 Guo, H., Jiang, F., Cheng, H. R., Simpson, I. J., Wang, X. M., Ding, A. J., Wang, T. J.,
739 Saunders, S. M., Wang, T., Lam, S. H. M., Blake, D. R., Zhang, Y. L., and Xie, M.:
740 Concurrent observations of air pollutants at two sites in the Pearl River Delta and the
741 implication of regional transport, Atmos. Chem. Phys., 9, 7343-7360, 2009.
742 Guo, H., Cheng, H. R., Ling, Z. H., Louie, P. K. K., and Ayoko, G. A.: Which emission
743 sources are responsible for the volatile organic compounds in the atmosphere of Pearl River
744 Delta? J. Hazard. Mater., 188, 116-124, 2011.

745 Guo, H., Ling, Z. H., Cheung, K., Jiang, F., Wang, D. W., Simpson, I. J., Barletta, B.,
746 Meinardi, S., Wang, T. J., Wang, X. M., Saunders, S. M., and Blake, D. R.: Characterization
747 of photochemical pollution at different elevations in mountainous areas in Hong Kong,
748 Atmos. Chem. Phys., 13, 3881-3898, 2013.
749 Guo, H., Ling, Z. H., Cheng, H. R., Simpson, I. J., Lyu, X. P., Wang, X. M., Shao, M., Lu, H.
750 X., Ayoko, G., Zhang, Y. L. and Saunders, S. M.: Tropospheric volatile organic compounds
751 in China, Sci. Total Environ., 574, 1021-1043, 2017.
752 Hong Kong Environmental Protection Department (HKEPD): Inquire and Download Air
753 Quality Monitoring Data, available at: epic.epd.gov.hk/ca/uid/airdata (last access: 25 October
754 2018), 2017a.
755 Hong Kong Environmental Protection Department (HKEPD): Cleaning the Air at Street
756 Level, available at: http://www.epd.gov.hk/epd/english/environmentinhk/air/prob_solutions
757 /strategies_apc.html (last access: 25 October 2018), 2017b.
758 Hong Kong Environmental Protection Department (HKEPD): Phasing Out Pre-Euro IV
759 Diesel Commercial Vehicles, available at: https://www.epd.gov.hk/epd/english
760 /environmentinhk/air/prob_solutions/Phasing_out_diesel_comm_veh.html (last access: 25
761 October 2018), 2018.
762 Hong Kong Observatory (HKO): Real-time Data Display from ENVF Atmospheric &
763 Environmental Database, available at: http://envf.ust.hk/dataview/hko_wc/current/ (last
764 access: 25 October 2018), 2017.
765 Huang, J. P., Fung, J. C., Lau, A. K., and Qin, Y.: Numerical simulation and process analysis
766 of typhoon-related ozone episodes in Hong Kong, J. Geophys. Res. Atmos., 110, D05301,
767 https://doi.org/10.1029/2004jd004914, 2005.
768 Jacob, D. J.: Introduction to atmospheric chemistry, Princeton University Press, Princeton,
769 New Jersey, 1999.

770 Jenkin, M. E., Saunders, S. M., and Pilling, M. J.: The tropospheric degradation of volatile
771 organic compounds: a protocol for mechanism development, Atmos. Environ., 31, 81-104,
772 1997.
773 Jenkin, M. E., Saunders, S. M., Wagner, V., and Pilling, M. J.: Protocol for the development
774 of the Master Chemical Mechanism, MCM v3 (Part B): tropospheric degradation of aromatic
775 volatile organic compounds, Atmos. Chem. Phys., 3, 181-193, 2003.
776 Jiang, F., Guo, H., Wang, T. J., Cheng, H. R., Wang, X. M., Simpson, I. J., Ding, A. J.,
777 Saunders, S. M., Lam, S. H. M., and Blake, D. R.: An ozone episode in the Pearl River Delta:
778 Field observation and model simulation, J. Geophys. Res., 115, D22305,
779 https://doi.org/10.1029/2009JD013583, 2010.
780 Jiang, Y. C., Zhao, T. L., Liu, J., Xu, X. D., Tan, C. H., Cheng, X. H., Bi, X. Y., Gan, J. B.,
781 You, J. F., and Zhao, S. Z.: Why does surface ozone peak before a typhoon landing in
782 southeast China? Atmos. Chem. Phys., 15, 13331-13338, 2015.
783 Johnson, B.T.: Diesel engine emissions and their control, Platin. Met. Rev., 52, 23-37, 2008.
784 Kanaya, Y., Pochanart, P., Liu, Y., Li, J., Tanimoto, H., Kato, S., Suthawaree, J., Inomata, S.,
785 Taketani, F., Okuzawa, K., and Kawamura, K.: Rates and regimes of photochemical ozone
786 production over Central East China in June 2006: a box model analysis using comprehensive
787 measurements of ozone precursors, Atmos. Chem. Phys., 9, 7711-7723, 2009.
788 Kashdan, J.T.: Tracer LIF Visualisation Studies of Piston-Top Fuel Films in a Wall-Guided,
789 Low-NO_x Diesel Engine, SAE Tech. Paper, 2008-01-2474, 2008.
790 Lakey, P. S. J., George, I. J., Whalley, L. K., Baeza-Romero, M. T., and Heard, D. E.:
791 Measurements of the HO_2 uptake coefficients onto single component organic aerosols,
792 Environ. Sci. Technol., 49, 4878-4885, 2015.

793 Lam, K. S., Wang, T. J., Wu, C. L., and Li, Y. S.: Study on an ozone episode in hot season in
794 Hong Kong and transboundary air pollution over Pearl River Delta region of China, Atmos.
795 Environ., 39, 1967-1977, 2005.
796 Lam, S. H. M., Saunders, S. M., Guo, H., Ling, Z. H., Jiang, F., Wang, X. M., and Wang, T.
797 J.: Modelling VOC source impacts on high ozone episode days observed at a mountain
798 summit in Hong Kong under the influence of mountain-valley breezes, Atmos. Environ., 81,
799 166-176, 2013.
800 Lau, A. K. H., Yuan, Z., Yu, J. Z., and Louie, P. K.: Source apportionment of ambient
801 volatile organic compounds in Hong Kong, Sci. Total Environ., 408, 4138-4149, 2010.
802 Lee, E., Chan, C. K., and Paatero, P.: Application of positive matrix factorization in source
803 apportionment of particulate pollutants in Hong Kong, Atmos. Environ., 33, 3201-3212, 1999.
804 Lefohn, A. S., Shadwick, D. and Oltmans, S. J.: Characterizing changes in surface ozone
805 levels in metropolitan and rural areas in the United States for 1980–2008 and 1994–2008,
806 Atmos. Environ., 44, 5199-5210, 2010.
807 Lin, M., Horowitz, L.W., Payton, R., Fiore, A. M., and Tonnesen, G.: US surface ozone
808 trends and extremes from 1980 to 2014: quantifying the roles of rising Asian emissions,
809 domestic controls, wildfires, and climate, Atmos. Chem. Phys., 17, 2943-2970, 2017.
810 Ling, Z. H. and Guo, H.: Contribution of VOC sources to photochemical ozone formation
811 and its control policy implication in Hong Kong, Environ. Sci. Policy, 38, 180-191, 2014.
812 Ling, Z. H., Guo, H., Cheng, H. R., and Yu, Y. F.: Sources of ambient volatile organic
813 compounds and their contributions to photochemical ozone formation at a site in the Pearl
814 River Delta, southern China, Environ. Pollut., 159, 2310-2319, 2011.
815 Ling, Z. H., Guo, H., Zheng, J. Y., Louie, P. K. K., Cheng, H. R., Jiang, F., Cheung, K.,
816 Wong, L. C., and Feng, X. Q.: Establishing a conceptual model for photochemical ozone
817 pollution in subtropical Hong Kong, Atmos. Environ., 76, 208–220, 2013.

Ling, Z. H., Guo, H., Lam, S. H. M., Saunders, S. M., and Wang, T.: Atmospheric photochemical reactivity and ozone production at two sites in Hong Kong: Application of a Master Chemical Mechanism-photochemical box model, J. Geophys. Res. Atmos., 119, 10567-10582, 2014.

Ling, Z., Guo, H., Simpson, I. J., Saunders, S. M., Lam, S. H. M., Lyu, X., and Blake, D. R.: New insight into the spatiotemporal variability and source apportionments of C_1–C_4 alkyl nitrates in Hong Kong, Atmos. Chem. Phys., 16, 8141-8156, 2016a.

Ling, Z., Guo, H., Chen, G., Lam, S. H. M., and Fan, S.: Formaldehyde and acetaldehyde at different elevations in mountainous areas in Hong Kong, Aerosol Air Qual. Res., 16, 1868-1878, 2016b.

Liu, Y., Shao, M., Lu, S. H., Chang, C. C., Wang, J. L., and Chen, G.: Volatile Organic Compound (VOC) measurements in the Pearl River Delta (PRD) region, China, Atmos. Chem. Phys., 8, 1531-1545, 2008.

Liu, Z., Wang, Y., Gu, D., Zhao, C., Huey, L. G., Stickel, R., Liao, J., Shao, M., Zhu, T., Zeng, L., and Amoroso, A.: Summertime photochemistry during CAREBeijing-2007: RO_x budgets and O_3 formation, Atmos. Chem. Phys., 12, 7737-7752, 2012.

Lyu, X. P., Ling, Z. H., Guo, H., Saunders, S. M., Lam, S. H. M., Wang, N., Wang, Y., Liu, M., and Wang, T.: Re-examination of C_1-C_5 alkyl nitrates in Hong Kong using an observation-based model, Atmos. Environ., 120, 28-37, 2015.

Lyu, X. P., Liu, M., Guo, H., Ling, Z. H., Wang, Y., Louie, P. K. K., and Luk, C. W. Y.: Spatiotemporal variation of ozone precursors and ozone formation in Hong Kong: grid field measurement and modelling study, Sci. Total Environ., 569, 1341-1349, 2016a.

Lyu, X. P., Guo, H., Simpson, I. J., Meinardi, S., Louie, P. K. K., Ling, Z. H., Wang, Y., Liu, M., Luk, C. W. Y., Wang, N., and Blake, D. R.: Effectiveness of replacing catalytic

converters in LPG-fuelled vehicles in Hong Kong, Atmos. Chem. Phys., 16, 6609-6626, 2016b.

Lyu, X. P., Chen, N., Guo, H., Zhang,W. H., Wang, N.,Wang, Y., and Liu, M.: Ambient volatile organic compounds and their effect on ozone production in Wuhan, Central China, Sci. Total Environ., 541, 200-209, 2016c.

Lyu, X. P., Zeng, L. W., Guo, H., Simpson, I. J., Ling, Z. H., Wang, Y., Murray, F., Louie, P. K. K., Saunders, S. M., Lam, S. H. M., and Blake, D. R.: Evaluation of the effectiveness of air pollution control measure in Hong Kong, Environ. Pollut., 220, 87-94, 2017a.

Lyu, X. P., Guo, H., Wang, N., Simpson, I. J., Cheng, H. R., Zeng, L. W., Saunders, S. M., Lam, S. H. M., Meinardi, S., and Blake, D. R.: Modeling C_1-C_4 alkyl nitrate photochemistry and their impacts on O_3 production in urban and suburban environments of Hong Kong, J. Geophys. Res. Atmos., 122, 10539-10556, 2017b.

Madronich, S. and Flocke, S.: The role of solar radiation in atmospheric chemistry, Environ. Photochem., 1-26, 1999.

Ministry of Ecology and Environment of the People's Republic of China (MEE PRC): Action plan for preventing and controlling air pollution in Guangdong Province, China, available at: http://www.mee.gov.cn/xxgk/hjyw/201403/t20140303_268619.shtml (last access: 25 October 2018), 2014.

NARSTO: An Assessment of tropospheric ozone pollution: a North American perspective, NARSTO synthesis team, available at: http://cdiac.ess-dive.lbl.gov /programs/NARSTO/ozone_assessment.html (last access: 25 October 2018), 2000.

National Research Council (NRC): Rethinking the ozone problem in urban and regional air pollution, National Academies Press, 1992.

865 Norris, G., Wade, K., and Foley, C.: EPA Positive Matrix Factorization (PMF) 3.0
866 Fundamentals & User Guide, EPA 600/R-08/108, US Environmental Protection Agency,
867 Office of Research and Development, Washington, 2008.
868 Norris, G., Duvall, R., Brown, S., and Song, B.: EPA Positive Matrix Factorization (PMF)
869 5.0 Fundamentals & User Guide, EPA 600/R-14/108, US Environmental Protection Agency,
870 Office of Research and Development, Washington, 2014.
871 Ou, J.M., Guo, H., Zheng, J.Y., Cheung, K., Louie, P.K.K., Ling, Z.H., and Wang, D.W.:
872 Concentrations and sources of non-methane hydrocarbons (NMHCs) from 2005 to 2013 in
873 Hong Kong: A multi-year real-time data analysis. Atmos. Environ., 103, 196-206, 2015.
874 Paatero, P.: Least squares formulation of robust non-negative factor analysis, Chemometr.
875 Intell. Lab., 37, 23-35, 1997.
876 Paatero, P.: User's Guide for Positive Matrix Factorization Programs PMF2 and PMF3, Part
877 1: Tutorial, Prepared by University of Helsinki, Finland (February), 2000a.
878 Paatero, P.: User's Guide for Positive Matrix Factorization Programs PMF2 and PMF3, Part
879 2: Reference, Prepared by University of Helsinki, Finland, 2000b.
880 Parrish, D. D., Lamarque, J. F., Naik, V., Horowitz, L., Shindell, D. T., Staehelin, J., Derwent,
881 R., Cooper, O. R., Tanimoto, H., Volz-Thomas, A., and Gilge, S.: Long-term changes in
882 lower tropospheric baseline ozone concentrations: Comparing chemistry-climate models and
883 observations at northern midlatitudes., J. Geophys. Res. Atmos., 119, 5719-5736, 2014.
884 Polissar, A. V., Hopke, P. K., Paatero, P., Malm, W. C., and Sisler, J. F.: Atmospheric aerosol
885 over Alaska: 2. Elemental composition and sources, J. Geophys. Res. Atmos., 103, D15,
886 19045-19057, 1998.
887 Reff, A., Eberly, S. I., and Bhave, P. V.: Receptor modeling of ambient particulate matter
888 data using positive matrix factorization: review of existing methods, J. Air Waste Manag.
889 Assoc., 57, 146-154, 2007.

890 Richter, A., Burrows, J.P. Nub, H., Granier, C., and Niemeier, U.: Increase in tropospheric
891 nitrogen dioxide over China observed from space, Nature, 437, 129, 2005.
892 Sahoo, D., Petersen, B., and Miles, P.: Measurement of equivalence ratio in a light-duty low
893 temperature combustion diesel engine by planar laser induced fluorescence of a fuel tracer,
894 SAE Int. J. Engines, 4, 2312-2325, 2011.
895 Saunders, S. M., Jenkin, M. E., Derwent, R. G., and Pilling, M. J.: Protocol for the
896 development of the Master Chemical Mechanism, MCM v3 (Part A): tropospheric
897 degradation of non-aromatic volatile organic compounds, Atmos. Chem. Phys., 3, 161-180,
898 2003.
899 Schauer, J. J., Kleeman, M. J., Cass, G. R., and Simoneit, B. R.: Measurement of emissions
900 from air pollution sources. 2. C_1 through C_{30} organic compounds from medium duty diesel
901 trucks, Environ. Sci. Technol., 33, 1578-1587, 1999.
902 Sillman, S.: The relation between ozone, NO_x and hydrocarbons in urban and polluted rural
903 environments, Atmos. Environ., 33, 1821-1845, 1999.
904 Simpson, I. J., Blake, N. J., Barletta, B., Diskin, G. S., Fuelberg, H. E., Gorham, K., Huey, L.
905 G., Meinardi, S., Rowland, F. S., Vay, S. A., Weinheimer, A. J., Yang, M., and Blake, D. R.:
906 Characterization of trace gases measured over Alberta oil sands mining operations: 76
907 speciated C_2-C_{10} volatile organic compounds (VOCs), CO_2, CH_4, CO, NO, NO_2, NO_y, O_3 and
908 SO_2, Atmos. Chem. Phys., 10, 11931−11954, 2010.
909 So, K. L. and Wang, T.: On the local and regional influence on ground-level ozone
910 concentrations in Hong Kong, Environ. Pollut., 123, 307-317, 2003.
911 United States Environmental Protection Agency (US EPA): Positive Matrix Factorization
912 Model for environmental data analyses, available at https://www.epa.gov/air-
913 research/positive-matrix-factorization-model-environmental-data-analyses (last access: 25
914 October 2018), 2017.

915 Wang, H., Lyu, X. P., Guo, H., Wang, Y., Zou, S. C., Ling, Z. H., Wang, X. M., Jiang, F.,
916 Zeren, Y. Z., Pan, W. Z., Huang X. B., and Shen, J.: Ozone pollution around a coastal region
917 of South China Sea: Interaction between marine and continental air, Atmos. Chem. Phys., 18,
918 4277-4295, 2018b.
919 Wang, H. X., Kiang, C. S., Tang, X. Y., Zhou, X. J., and Chameides, W. L.: Surface ozone:
920 A likely threat to crops in Yangtze delta of China, Atmos. Environ., 39, 3843-3850, 2005.
921 Wang, N., Guo, H., Jiang, F., Ling, Z. H., and Wang, T.: Simulation of ozone formation at
922 different elevations in mountainous area of Hong Kong using WRF-CMAQ model, Sci. Total
923 Environ, 505, 939-951, 2015.
924 Wang, T., Wu, Y. Y., Cheung, T. F. and Lam, K. S.: A study of surface ozone and the
925 relation to complex wind flow in Hong Kong, Atmos. Environ., 35, 3203-3215, 2001.
926 Wang, T., Wei, X. L., Ding, A. J., Poon, S. C., Lam, K. S., Li, Y. S., Chan, L. Y., and Anson,
927 M.: Increasing surface ozone concentrations in the background atmosphere of Southern China,
928 1994-2007, Atmos. Chem. Phys., 9, 6217-6227, 2009.
929 Wang, T., Xue, L. K., Brimblecombe, P., Lam, Y. F., Li, L., and Zhang, L.: Ozone pollution
930 in China: A review of concentrations, meteorological influences, chemical precursors, and
931 effects, Sci. Total Environ., 575, 1582-1596, 2017b.
932 Wang, Y., Wang, H., Guo, H., Lyu, X. P., Cheng, H. R., Ling, Z. L., Louie, P. K. K.,
933 Simpson, I J., Meinardi, S., and Blake, D. R.: Long-term O_3- precursor relationships in Hong
934 Kong: field observation and model simulation, Atmos. Chem. Phys., 17, 10919-10935, 2017a.
935 Wang, Y., Guo, H., Zou, S. C., Lyu, X. P., Ling, Z. H., Cheng, H. R., and Zeren, Y. Z.:
936 Surface O_3 photochemistry over the South China Sea: Application of a near-explicit chemical
937 mechanism box model, Environ. Pollut., 234, 155-166, 2018a.
938 Willmott, C. J.: Some comments on the evaluation of model performance., B. Am. Meteorol.
939 Soc., 63, 1309-1313, 1982.

940 Xu, X., Lin, W., Wang, T., Yan, P., Wang, J., Meng, Z., and Wang, Y.: Long-term trend of
941 surface ozone at a regional background station in eastern China 1991-2006: enhanced
942 variability, Atmos. Chem. Phys., 8, 2595-2607, 2008.
943 Xu, Z., Wang, T., Wu, J., Xue, L., Chan, J., Zha, Q., Zhou, S., Louie, P. K., and Luk, C. W.:
944 Nitrous acid (HONO) in a polluted subtropical atmosphere: Seasonal variability, direct
945 vehicle emissions and heterogeneous production at ground surface, Atmos. Environ., 106,
946 100-109, 2015.
947 Xue, L. K., Wang, T., Louie, P. K., Luk, C. W., Blake, D. R., and Xu, Z.: Increasing external
948 effects negate local efforts to control ozone air pollution: a case study of Hong Kong and
949 implications for other Chinese cities, Environ. Sci. Technol., 48, 10769-10775, 2014a.
950 Xue, L. K., Wang, T., Gao, J., Ding, A. J., Zhou, X. H., Blake, D. R., Wang, X. F., Saunders,
951 S. M., Fan, S. J., Zuo, H. C., and Zhang, Q. Z.: Ground-level ozone in four Chinese cities:
952 precursors, regional transport and heterogeneous processes, Atmos. Chem. Phys., 14, 13175-
953 13188, 2014b.
954 Xue, L. K., Gu, R. R., Wang, T., Wang, X. F., Saunders, S., Blake, D., Louie, P. K. K., Luk,
955 C. W. Y., Simpson, I., Xu, Z., Wang, Z., Gao, Y., Lee, S. C., Mellouki, A., and Wang, W. X.:
956 Oxidative capacity and radical chemistry in the polluted atmosphere of Hong Kong and Pearl
957 River Delta regional analysis of a severe photochemical smog episode, Atmos. Chem., Phys.,
958 16, 9891-9903, 2016.
959 Yao, C., Cheung, C. S., Cheng, C., Wang, Y., Chan, T. L., and Lee, S. C.: Effect of
960 diesel/methanol compound combustion on diesel engine combustion and emissions, Energy
961 Convers. Manag., 49, 1696-1704, 2008.
962 Yao, D., Lyu, X., Murray, F., Morawska, L., Yu, W., Wang, J., and Guo, H.: Continuous
963 effectiveness of replacing catalytic converters on liquified petroleum gas-fueled vehicles in
964 Hong Kong., Sci. Total Environ., 648, 830-838, 2019.

965 Zeng, L., Lyu, X., Guo, H., Zou, S., and Ling, Z.: Photochemical Formation of C_1–C_5 Alkyl
966 Nitrates in Suburban Hong Kong and over the South China Sea, Environ. Sci. Technol., 52,
967 5581-5589, 2018.
968 Zhang, J., Wang, T., Chameides, W. L., Cardelino, C., Kwok, J., Blake, D. R., Ding, A., and
969 So, K. L.: Ozone production and hydrocarbon reactivity in Hong Kong, Southern China,
970 Atmos. Chem. Phys., 7, 557-573, 2007.
971 Zhang, Y., Wang, X., Blake, D.R., Li, L., Zhang, Z., Wang, S., Guo, H., Lee, S.C., Gao, B.,
972 Chan, L., and Wu, D.: Aromatic hydrocarbons as ozone precursors before and after outbreak
973 of the 2008 financial crisis in the Pearl River Delta region, south China., J. Geophys. Res.
974 Atmos., 117, D15306, https://doi.org/10.1029/2011JD017356, 2012.
975 Zheng, B., Tong, D., Li, M., Liu, F., Hong, C., Geng, G., Li, H., Li, X., Peng, L., Qi, J., and
976 Yan, L.: Trends in China's anthropogenic emissions since 2010 as the consequence of clean
977 air actions., Atmos. Chem. Phys., 18, 14095-14111, 2018.